



**HAL**  
open science

## **Project Coolbit: can your watch predict heat stress and thermal comfort sensation?**

Negin Nazarian, Sijie Liu, Manon Kohler, Jason K W Lee, Clayton Miller, Winston T L Chow, Sharifah Badriyah Alhadad, Alberto Martilli, Matias Quintana, Lindsey Sunden, et al.

### **► To cite this version:**

Negin Nazarian, Sijie Liu, Manon Kohler, Jason K W Lee, Clayton Miller, et al.. Project Coolbit: can your watch predict heat stress and thermal comfort sensation?. *Environmental Research Letters*, 2020, 16 (3), pp.034031. 10.1088/1748-9326/abd130 . hal-03271125

**HAL Id: hal-03271125**

**<https://hal.science/hal-03271125>**

Submitted on 25 Jun 2021

**HAL** is a multi-disciplinary open access archive for the deposit and dissemination of scientific research documents, whether they are published or not. The documents may come from teaching and research institutions in France or abroad, or from public or private research centers.

L'archive ouverte pluridisciplinaire **HAL**, est destinée au dépôt et à la diffusion de documents scientifiques de niveau recherche, publiés ou non, émanant des établissements d'enseignement et de recherche français ou étrangers, des laboratoires publics ou privés.

ACCEPTED MANUSCRIPT • OPEN ACCESS

## Project Coolbit: Can your watch predict heat stress and thermal comfort sensation?

To cite this article before publication: Negin Nazarian *et al* 2020 *Environ. Res. Lett.* in press <https://doi.org/10.1088/1748-9326/abd130>

### Manuscript version: Accepted Manuscript

Accepted Manuscript is “the version of the article accepted for publication including all changes made as a result of the peer review process, and which may also include the addition to the article by IOP Publishing of a header, an article ID, a cover sheet and/or an ‘Accepted Manuscript’ watermark, but excluding any other editing, typesetting or other changes made by IOP Publishing and/or its licensors”

This Accepted Manuscript is © 2020 The Author(s). Published by IOP Publishing Ltd.

As the Version of Record of this article is going to be / has been published on a gold open access basis under a CC BY 3.0 licence, this Accepted Manuscript is available for reuse under a CC BY 3.0 licence immediately.

Everyone is permitted to use all or part of the original content in this article, provided that they adhere to all the terms of the licence <https://creativecommons.org/licenses/by/3.0>

Although reasonable endeavours have been taken to obtain all necessary permissions from third parties to include their copyrighted content within this article, their full citation and copyright line may not be present in this Accepted Manuscript version. Before using any content from this article, please refer to the Version of Record on IOPscience once published for full citation and copyright details, as permissions may be required. All third party content is fully copyright protected and is not published on a gold open access basis under a CC BY licence, unless that is specifically stated in the figure caption in the Version of Record.

View the [article online](#) for updates and enhancements.

# Project Coolbit: Can your Watch Predict Heat Stress and Thermal Comfort Sensation?

Negin Nazarian<sup>\*1,2</sup>, Sijie Liu<sup>1</sup>, Manon Kohler<sup>3</sup>, Jason K. W. Lee<sup>3</sup>, Clayton Miler<sup>3</sup>, Winston Chow<sup>3,6</sup>, Sharifah Badriyah Alhadad<sup>3</sup>, Alberto Martilli<sup>4</sup>, Matias Quintana<sup>3</sup>, Lindsey Sunden<sup>5</sup>, and Leslie Norford<sup>7,8</sup>

<sup>1</sup>University of New South Wales, Sydney, Australia

<sup>2</sup>ARC Centre of Excellence for Climate Extremes, UNSW Sydney 2052, Australia

<sup>3</sup>National University of Singapore, Singapore

<sup>4</sup>Center for Research on Energy, Technology and Environment (CIEMAT), Madrid, Spain

<sup>5</sup>Fitbit, Inc., San Francisco, USA

<sup>6</sup>Singapore Management University, Singapore

<sup>7</sup>Department of Architecture, Massachusetts Institute of Technology, USA

<sup>8</sup>Singapore-MIT Alliance for Research and Technology, Singapore

November 15, 2020

## Abstract

Global climate is changing as a result of anthropogenic warming, leading to higher daily excursions of temperature in cities. Such elevated temperatures have great implications on human thermal comfort and heat stress, which should be closely monitored. Current methods for heat exposure assessments (surveys, microclimate measurements, and laboratory experiments), however, present several limitations: measurements are scattered in time and space and data gathered on outdoor thermal stress and comfort often does not include physiological and behavioral parameters. To address these shortcomings, Project Coolbit aims to introduce a human-centric approach to thermal comfort assessments. In this study, we propose and evaluate the use of wrist-mounted wearable devices to monitor environmental and physiological responses that span a wide range of spatial and temporal distributions. We introduce an integrated wearable weather station that records a) microclimate parameters (such as air temperature and humidity), b) physiological parameters (heart rate, skin temperature and humidity), and c) subjective feedback. The feasibility of this methodology to assess thermal comfort and heat stress is then evaluated using two sets of experiments: controlled-environment physiological data collection, and outdoor environmental data collection. We find that using the data obtained through the wrist-mounted wearables, core temperature can be predicted non-invasively with 95 percent of target attainment (PTA) within  $\pm 0.27^\circ\text{C}$ . Additionally, a direct connection between the air temperature at the wrist ( $T_{a,w}$ ) and the perceived activity level (PAV) of individuals was drawn. We observe that with increased  $T_{a,w}$ , the desire for physical activity is significantly reduced, reaching "Transition only" PAV level at  $36^\circ\text{C}$ . These assessments reveal that the wearable methodology provides a comprehensive and accurate representation of human heat exposure, which can be

\*Corresponding author. n.nazarian@unsw.edu.au. #2045 Red Centre West Wing (H13), UNSW Sydney, NSW 2052 Australia.

extended in real-time to cover a large spatial distribution in a given city and quantify the impact of heat exposure on human life.

## 1 Introduction

Heat exposure directly impacts our wellbeing, productivity, and cognitive performance [1, 2] and presents an increasing concern to human health in the face of global climate change [3, 4]. Urban areas are particularly vulnerable to the impacts of heat, as they concentrate large numbers of vulnerable people (such as young children, elderly, and those with existing physical and mental health conditions [5]) in settings where ambient temperatures are often higher than suburban and rural areas (Urban Heat Island effect [6]). The combined effect is detrimental to the health of urban residents. Heat mortality is referred to as “private and silent deaths” and even in developed countries such as Australia and the United States, heatwaves are reported to kill more than any other natural disaster [5, 7, 8]. Therefore, it is paramount that we deeply understand and closely monitor not only the climatic factors but also the personalized responses of the population to assess the impact of urban heat exposure on human health and wellbeing.

Currently, measurements for thermal comfort and heat stress are done through two main methods: 1) measurements of microclimate and physiological parameters, commonly in fixed locations or laboratory settings, and 2) surveys of human sensation in response to thermal environments [9–14]. Although the information gathered contributes significantly to our knowledge of thermal comfort, several limitations persist:

1. Measurements are scattered in time and space. The spatial and temporal distributions of thermal environment and comfort in the city are not readily available through the experiments and have been mainly achieved by numerical modeling [15–19].
2. Data gathered on thermal comfort often do not include the “human factor,” i.e. physiological and behavioral parameters corresponding to the thermal comfort of individuals, despite the fact that the response and vulnerability to thermal environments vary greatly between individuals [20–22].
3. Data gathered on heat stress often do not represent realistic conditions in urban environments and are not obtained in real-time. For instance, the majority of temperature-mortality/-morbidity relations are drawn based on temperatures recorded at fixed monitoring stations [23], which may not resemble what people experience as they go about their lives in the city.

Project Coolbit is motivated by the challenges and limitations of existing methods. Innovative methods of obtaining data are needed to a) span larger spatial and temporal distributions in cities, b) obtain real-time, unsupervised, and non-intrusive data on thermal comfort and heat stress in the built environment, and c) provide human-centric assessments, such that we extend previous approaches to thermal comfort and heat stress.

These objectives can be achieved through crowd-sourced monitoring as opposed to centralized experimentations. Crowdsourcing or ubiquitous sensing (i.e. obtaining data by using a distributed number of sensors) has recently become feasible due to the rapidly growing number of affordable internet-enabled sensing devices [24]. Among these, wearable technologies represent a range of opportunities for comfort and health assessments. These devices enable us to generate a significant amount of data about people’s immediate en-

1  
2  
3 vironments, add behavioral and physiological components [25, 26], and approach thermal comfort and heat  
4 stress as “human-centric” as opposed to “one-size-fits-all”. Additionally, wearables travel with the individu-  
5 als in realistic exposure scenarios and, therefore, data collected by wearables combined with GPS data can  
6 provide a spatiotemporal distribution of environmental parameters and individual’s exposure. However, to  
7 date, there is no wearable sensing (neither commercial nor in academic use) available nor tested that can  
8 combine all the parameters relevant to thermal comfort and heat stress. Accordingly, we propose and test a  
9 methodology based on wearable devices here, which can ultimately enable a comprehensive yet unsupervised  
10 and non-invasive assessment of thermal comfort and heat stress in the built environment.

11  
12  
13  
14 The current generation of wearables monitors such physiological parameters as heart rate, which helps under-  
15 stand various aspects of human wellbeing and health including sleep quality. However, to assess thermal stress  
16 and comfort, the measurements should be extended. Human skin is the mediator between the environment  
17 and human body and, therefore, skin temperature and conductance play a major role in thermoregulatory  
18 processes involved in thermal comfort and heat stress [27, 28]. Sim et al. [28] showed that wrist skin tem-  
19 peratures can be used to predict whole-body thermal sensation. Additionally, several studies have used heart  
20 rate data to indicate thermal stress in the built environment. A study by Buller et al. 2013 introduced a  
21 non-invasive and continuous method of estimating the human core temperature, the main factor in determin-  
22 ing heat stress, from sequential heart rate observations. They showed that out of 52,000 observations, 95%  
23 of all core temperature estimates fell within  $\pm 0.63^{\circ}C$  of measurements. This, in addition to the advancement  
24 of ubiquitous sensing in the built environment, has opened new doors to use wearables for thermal exposure  
25 assessments. Nonetheless, this is an emerging field and there are only a handful of studies that investigate  
26 wearable solutions [16, 25, 26, 30]. Among these, Nakayoshi et al. [25] represents a comprehensive measure-  
27 ment of thermal comfort, monitoring four relevant environmental parameters in the proximity of the human  
28 body as well as physiological responses (heart rate and skin temperature) and subjective feedback, and found  
29 a correlation between skin temperature and thermal comfort index in a semi-controlled testing environment.  
30 The wearable system involved five sensing units worn by the participants on multiple locations: hat, belt,  
31 hand, and forehead skin, and carried in a small sash. Although comprehensive for research purposes, this  
32 methodology cannot be employed in unsupervised settings and is considered impractical for implementation  
33 in real-life applications. Wrist-mounted wearables can address such concerns regarding scalability in realistic  
34 applications, particularly as smartwatches have recently dominated the wearable tech worldwide [31]. How-  
35 ever, the challenges of using wearables as sensing methodologies are still numerous and, to date, reliability of  
36 wrist-mounted wearable data collection under dynamic use are not fully assessed. There is an urgent need to  
37 quantitatively assess the performance of wearables for heat exposure monitoring, which motivates the present  
38 study. Here, we propose an Integrated Wearable Weather Station for unsupervised assessment of urban heat  
39 impact on individuals (Sec 2.1), and further discuss experiments that rigorously assess the feasibility of this  
40 methodology for various heat exposure evaluations in the built environment (Sec. 2.2). In Secs. 3.1 and  
41 3.2, we evaluate the prediction of body core temperature (as the main predictor of heat stress) and thermal  
42 comfort sensation using collected data and lastly, we discuss the implication of these findings as well as future  
43 research that can extend this methodology for real-time and unsupervised evaluation of urban heat impacts  
44 on human life in Sec. 4.

## 2 Methodology

### 2.1 Integrated Wearable Weather Station: Human-Centric Assessment of Thermal Comfort and Heat Stress

Innovative methods of obtaining data are needed to assess dynamic exposure to thermal environments in cities in a human-centric way. However, the assessment of thermal exposure is notoriously complex as it requires consideration of three critical components: a) environmental factors, b) physiological thermoregulation mechanisms of the human body, and c) subjective psychological perceptions and behavioral patterns as well as cultural and climatic backgrounds of individuals. Accordingly, the integration of all these components into one sensing unit hasn't been accomplished so far.

Unprecedented potentials are now emerging through the rise of Internet-of-Things sensing and wearable technologies for fitness, performance, and health tracking. Various wearable sensors have enabled continuous and real-time monitoring of physiological parameters over the last few years, with limited attention given to thermal exposure assessments [32–34]. Smart devices further provide interfaces for continuous interaction with users and data collection regarding behavioral patterns of human activities. Tapping on these emerging potentials, we propose wrist-mounted smart wearable devices as a novel approach to obtaining dynamic (spatially and temporally variable) data on thermal exposure. Integrated Wearable Weather Stations (Fig. 1) proposed here aim to record 1) microclimate parameters (such as air temperature and humidity) in the immediate environment of individuals, 2) physiological responses to heat (including heart rate, skin temperature and humidity), and 3) human activity and subjective feedback with regards to the thermal environment. Combined, this methodology aims to provide a comprehensive, integrated, and personalized assessment that improves our understanding of personal thermal comfort and heat stress in cities.



**Figure 1:** Schematic of an Integrated Wearable Weather Station for personalized assessment of urban heat exposure. In this format, three components of heat exposure are captured: 1) environmental parameters (such as air temperature, humidity, or radiation) are recorded on the outside of the strap (right image), 2) physiological response to heat exposure (including skin temperature and humidity) is captured based on sensors placed on the inner strap (left image), and 3) the smartwatch app is used to monitor activity level, location, and individuals' momentary assessment of heat exposure (center).

As the first example of a wearable weather station for heat exposure assessments, we employed Fitbit smartwatches [35] worn on the wrist that are equipped with the **PurePulse (photoplethysmography) technology** for

1  
2  
3 134 heart rate monitoring [36, 36, 37]. The Fitbit smartwatches are then equipped with two coin-sized iButton  
4 135 environmental sensors (i.e. wireless data logger in the form of a 1.3 cm radius stainless steel button [38]),  
5 136 which are placed at the inner and outer face of the watch strap to collect temperature and humidity of air and  
6 137 skin. The iButton Hygrochron temperature/humidity data loggers (DS1923) are attached to the Fitbit devices  
7 138 with a 3D printed harness (Fig. 2) and measure the air/skin temperature and humidity ranging between -20  
8 139 to 85°C and 0 to 100% with  $\pm 0.5^\circ\text{C}$  and  $\pm 0.6\%$  accuracy, respectively. The use of the smartwatch app for  
9 140 obtaining subjective feedback was also assessed in a separate study (preliminary work presented by Jayathissa  
10 141 et al. [39]). The feasibility of such integrated sensing for inferring the personalized heat exposure in the built  
11 142 environment is assessed in Sec. 2.2.

15 **Figure 2:** Fitbit Ionic and sensor attachments deployed here  
16 17 for monitoring of a) temperature and humidity of air in the  
18 19 proximity of human body, b) heart rate, skin temperature, and  
20 21 humidity at wrist, and c) activity level and momentary feed-  
22 23 back. Two iButton sensors [38] are placed on the watch strap  
24 25 using a 3D printed harness. The Fitbit activity trackers used  
26 27 have a 3-axis accelerometer to track the wearer's motion pat-  
28 29 terns (e.g. those that indicate walking, swimming or cycling)  
30 31 to approximate the number of steps taken, calories burned,  
32 33 floor climbed, and length of time performing exercises. The  
34 35 PurePulse (photoplethysmography) technology for heart rate  
36 37 monitoring [36, 36, 37] uses LED lights installed at the back  
38 39 of the instrument to detect blood volume changes that are due  
40 41 to capillary expansion and contractions, and has been shown  
42 43 to tracks heart rate well when compared to three-lead electro-  
44 45 cardiography [37]. The design and use of the smartwatch app  
46 47 will be further discussed in future studies.



## 142 143 2.2 Experimental Campaigns: Assessing the Robustness of Data Collection using 144 145 Wrist-mounted Devices

146 Detailed measurements are carried out and compared with conventional sensing methods to investigate the  
147 148 accuracy of physiological and environmental data collected by wearables. We conducted two sets of experi-  
149 150 ments: 1) controlled-environment experiments in a climate chamber, and 2) semi-controlled experiments in a  
151 152 range of indoor-outdoor built environments. In the first experiment, the environmental conditions were kept  
153 154 unchanged while the metabolic rate was varied based on activity level, while the second experiment focused  
155 156 on the changes in the heat exposure and thermal comfort based on microclimate characteristics. The detailed  
157 158 setup and specification of each experiment are discussed here. Ethics approval for conducting human subject  
159 160 research was received from NUS Institutional Review Boards (Reference code N-18-071).

### 153 2.2.1 Controlled-Environment Test in the Climate Chamber

154 We conducted controlled-environment experiments in a climate chamber (Fig. 3) at the Department of Phys-  
155 156 iology of the National University of Singapore. These experiments aim to collect physiological responses to  
157 158  
159 160

heat (such as heart rate and skin temperature and humidity at the wrist) and further evaluate the relationship between wearable data and the body core temperature as the main indicator for heat strain [29].

**Figure 3:** Controlled-environment experiment at NUS Department of Physiology. A participant is walking on a treadmill while wearing the wrist-mounted sensor arrangement (Fig. 2), chest-wrapped heart rate monitoring (Polar A300), and iButton sensors for recording skin temperature at various body parts. The environmental parameters in the climate chamber as well as ratings of thermal sensation (ASHRAE's 7-point scale) and RPE are continuously monitored throughout the experiment. Data from the ingested telemetric capsules were collected by the wireless data-recording devices and the body core temperature is monitored closely such that the experiment is ceased if the threshold of 40°C is reached.



For the assessment of body core temperature, participants were asked to ingest VitalSense telemetric capsules [40] 8 to 10 hours prior to the trial. For continuous monitoring of skin temperature ( $T_{sk}$ ), four iButtons were placed at four right-hand sides of each participant's body (chest, upper arm, thigh, and calf) which, in addition to the iButton attached to the Fitbit strap, provide the distribution and mean skin temperature of participants throughout the experiment [41]. Heart rate is continuously monitored by the watch, as well as the chest strap heart rate monitoring device. Fifteen participants (seven female and eight male) were recruited between the age of 18-45. To have a representative group, the participants were evenly distributed among three categories: 1) Singaporean (or those from a similar tropical climate), 2) acclimatized expatriates (> 3years stay), and non-acclimatized expatriates (0-6 months stay). During the experimental trial, participants went through a low to moderate exercise on a treadmill (Fig. 3) in a moderate environment resembling outdoor conditions in Singapore ( $T_a = 27 - 29^\circ C$ ,  $RH = 70 - 80\%$ ). The experiment consisted of three stages and the exercise intensity was specified using Rating of Perceived Exertion (RPE, Borg [42]). Borg's RPE scale ranges from 6 to 20, resembling "very light" to "extremely hard" and is subjective. In our experiment, the three stages of activity (each 15-minutes) corresponded to RPE of 8-9, 10-11 and 12-13 to induce "fairly light," "moderate," and "somewhat hard" efforts in individuals, respectively. Accordingly, although generally healthy adults were targeted, there was no required threshold level of fitness. The run/walk exercise on the treadmill in this experiment resulted in a change in the metabolic rate and therefore body core temperature, which is needed for assessment of this methodology in a range of daily human activities.

### 2.2.2 Semi-Controlled Environment Test in the Built Environment

We further conducted environmental monitoring campaigns to evaluate and compare the wrist-mounted sensor data with microclimate measurements at fixed locations and calibrate the subjective individual thermal sensation with objective environmental measurements. Semi-controlled environment tests were performed where participants walked through a predefined path (covering different built environment characteristics - Fig. 4), while passing through a network of sensors and answering thermal comfort surveys (Fig. 5).

Fifteen sessions were organized over six days in October - November (inter-monsoon period), distributed



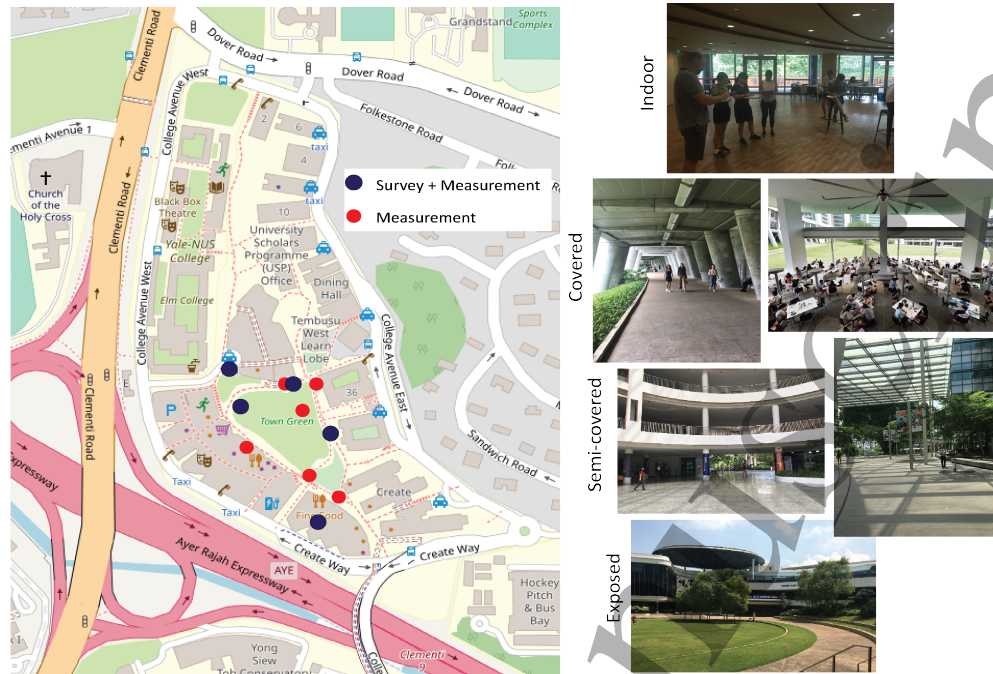


**Figure 4:** Map and photos of sensor network in the semi-controlled experiment. Left: map of the studied area at NUS UTown Campus with location of sensors and survey stations identified. Right: different characteristics of built environment selected for the experiment. Five survey stations were selected among an indoor (air-conditioned) environment, a semi-covered outdoor environment, covered outdoor locations (distinguished by a presence or lack thereof of ceiling fan), and fully exposed locations with different sky view factors.

over different hours of the day with approximately 40% conducted at noon and 20% each in the morning, afternoon, and evening. Sixty-two participants (with 48.2% female representation) were recruited for this study with age distribution of 19-48. Before the experiment, participants arrived at an indoor site and answered a questionnaire with regards to their personal profile (such as age, gender, and income level) as well as general preference towards the thermal environment. The project team then noted the participants' height, weight, and clothing level for the calculation of thermal comfort indices. Through this process, we also ensured that all participants have been in the same indoor environment for at least 30 minutes and have reached a physiologically stable condition before the start of the experiments. The profile of the participant group covered a body height range of 1.5-1.95m (mean 1.71m), weight of 42-102kg (mean 72kg), BMI of 18-32 (mean 23), and clothing insulation (iclo) of 0.34-0.44 (mean 0.36). Participants were then directed outdoors and asked to walk on a predefined path for approximately 40-50 minutes while wearing the modified wearable devices (Fig. 2). The path was chosen to cover a range of different built environment characteristics, including an indoor environment, a semi-covered outdoor environment, covered outdoor locations (distinguished by a presence or lack thereof of a ceiling fan), and fully exposed locations with different sky view factors. Along this path, participants passed two sets of fixed environmental sensors: 1) temperature and relative humidity sensors (Hobo MX2302 data logger) and 2) WBGT Heat Stress tracker (Kestrel 5400) to collect a comprehensive set of environmental data. The participants were then asked to answer the questionnaire at five pre-selected locations (i.e. survey stations equipped with environmental sensors). The survey asks participants to rank their thermal comfort satisfaction, sensation, and preference during the experiment using ASHRAE's 7-point

202 sensation and satisfaction scales as well as 3-point scale preference votes for various microclimate parameters  
 203 (temperature, humidity, wind speed, and radiation). Additionally, we continuously monitored participants'  
 204 heart rate, skin temperature, skin humidity, air temperature and humidity at wrist, location, and walking  
 205 speed during this experiment.



**Figure 5:** From left: sensor calibration in indoor laboratory; Hobo MX2302 temperature and humidity logger installed on site with a radiation shield; Kestrel 5400 Heat Stress Tracker at survey stations; and participants answering survey questions while wearing modified wearable devices. We ensured that the participants have been in Singapore for the week preceding the experiment (i.e. no overseas travels to hotter or colder climates that can affect their thermal sensation) and are well-rested to undertake a walk on flat terrain (40-50 minutes duration). Fixed environmental sensors are placed at the height of wearables at wrist (1.1 – 1.2 m).

## 3 Results

### 3.1 Physiological Data Collection and Prediction of Body Core Temperature

208 Here, we evaluate the physiological data collection using wearable sensors and their correlation with heat  
 209 strain (indicated by body core temperature). First, we compared the skin temperature obtained at the wrist  
 210 with temperature distribution at different body locations as well as air temperature (Fig. 6). **Chest and thigh**  
 211 exhibit the **highest skin temperature** ( $\sim 31\text{--}37^\circ\text{C}$ ), but also resemble body areas that were mostly covered by  
 212 participants. Skin temperature at the wrist ( $T_{s,w}$ ) shows the lowest median and minimum value compared to  
 213 **other body parts, while being consistently higher than the air temperature at wrist in the studied** conditions.  
 214 We observe that although the variability in ambient air temperature ( $T_a$ ) is very small ( $\sim 28\text{--}30^\circ\text{C}$ ), air  
 215 temperature at the wrist ( $T_{a,w}$ ) varies significantly during the experiment ( $\sim 26\text{--}34^\circ\text{C}$ ). This variation is due  
 216 to the sensor being placed at the proximity of the human body that acts as a heat source. This indicates that  
 217 air temperature at the wrist, alone, cannot determine the ambient air temperature in the built environment  
 218 as it exhibits the combined effect of environmental conditions ( $T_a$ ) and physiological responses ( $T_s$ ). However,  
 219 it is worth noting that it may be feasible to predict ambient air temperature using air and skin temperature  
 220 at the wrist considering the heat exchange between human skin surface and thermal environment [43, 44].  
 221 Additionally, we compared wrist skin temperature with mean skin temperature [41] for each participant (Fig.  
 222 6 - right) and found a **linear relationship for all participants**. The majority of participants, however, showed  
 223 lower wrist temperature compared to mean skin temperature, as temperatures at body extremities are usually  
 224 lower. Nonetheless, we observed that wrist (skin and air) temperatures ( $T_{a,w}$  and  $T_{s,w}$ ) better describe the  
 225 thermal comfort sensation of individuals (Sec. 3.2) and therefore these parameters are used for further analyses.  
 226 Further monitoring relative humidity at the wrist ( $RH_w$ ), we observe that for some participants,  $RH_w$  reaches

227 saturation during the experiments (in both controlled and semi-controlled settings). Although this value may  
 228 be higher than  $RH$  reported in other body parts due to the rubber wristband, we note that the onset of  
 229 sweating in different individuals (a critical determinant for the physiological strain and acclimatization) is  
 230 captured using the wearables which can be the subject for future research on personalized heat exposure.

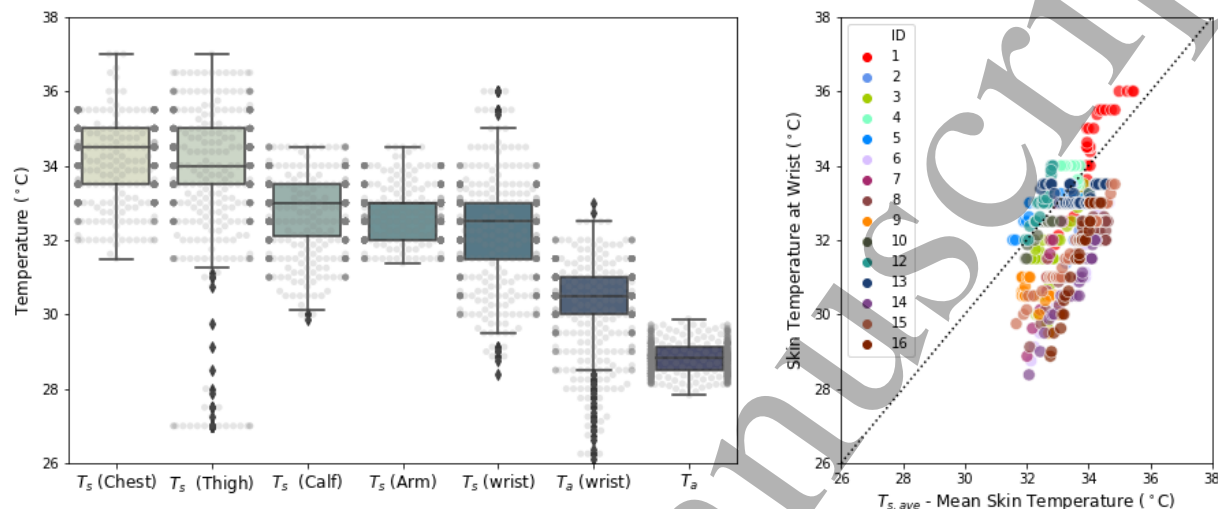


**Figure 6:** Left: Boxplots of observed skin temperature (1-min average) at five body areas (chest, thigh, calf, arm, and wrist) compared with air temperature measurements (near-wrist and ambient). Right: Distribution of skin temperature at wrist compared to mean body skin temperature for each individuals [41, 45]. Each ID represents a unique participant in the controlled-environment experiment and the 1:1 relationship is represented by a dashed line.

231 We further compared the wrist-mounted heart rate data with highly accurate measurements obtained from  
 232 chest strap sensors (Fig. 7 - left) as well as body core temperature obtained from telemetric capsules (Fig. 7  
 233 - right). The comparison is in agreement with previous studies that deemed Fitbit satisfactory for heart rate  
 234 monitoring [36]. We observed that 83% of heart rate data falls within the desired  $\pm 5$  bpm accuracy level, with  
 235 significantly smaller error observed for  $HR > 120$  that is particularly of interest for heat strain assessments.  
 236 Additionally, it is found that a significant majority of the error is attributed to two participants. After  
 237 evaluating temperature measurements at the wrist for these participants (not shown), we find that this error  
 238 has been introduced due to the way the smartwatches were worn during the experiment. This is particularly  
 239 important for future deployments and motivates means to ensure that wearables are worn correctly. An  
 240 example of such interventions can be a smartwatch function that monitors the wearable pressure on the wrist  
 241 and triggers an alarm on the smartwatch in response.

242 Lastly, we focused on non-invasive prediction of body core temperature ( $T_c$ ) using physiological and environ-  
 243 mental data by the wrist-mounted sensors. We observed that core temperature is positively correlated with  
 244 heart rate data (Fig. 7), which is in close agreement with the reported role of metabolic rate on heat strain [46].  
 245 However, given i) potential errors in heart rate monitoring using Fitbit watches (Fig. 7-left) and ii) moderate  
 246 performance in  $T_c$  prediction when only heart rate data are used [47, 48], we revisited the core temperature  
 247 predictions using sequential air and skin temperature at wrist ( $T_{a,w}$  and  $T_{s,w}$ ). A Kalman filter (also known as  
 248 linear quadratic estimation [49]) was employed to estimate core temperature ( $T_c$ ) using the variables obtained  
 249 from wearable sensors. The KF model (further explained in Appendix A) is used extensively for  $T_c$  estimation  
 250 using non-invasive measurements, mainly heart rate [47, 50–52].

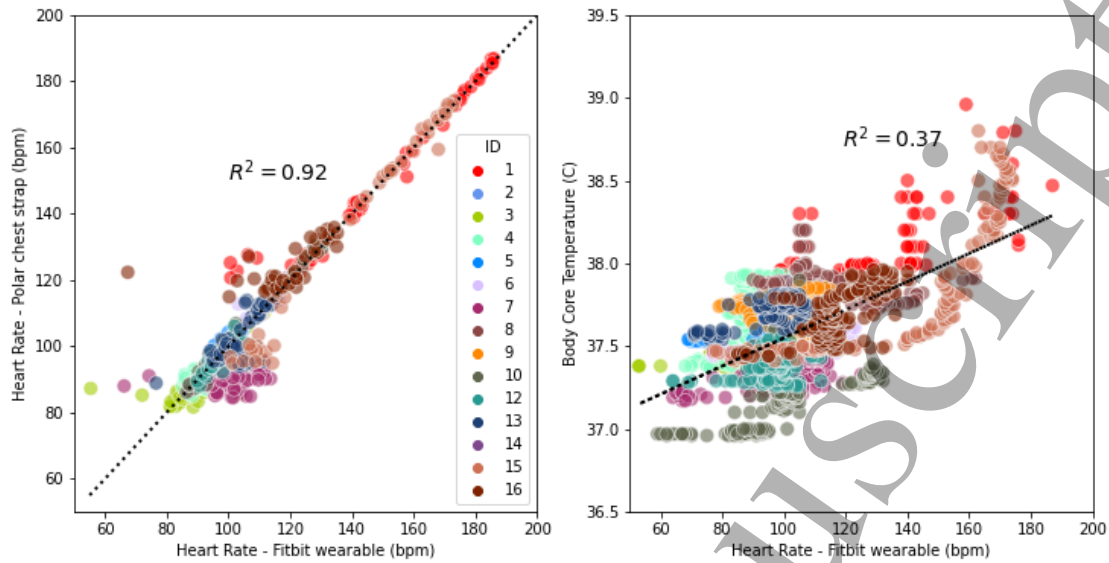


**Figure 7:** Left: Comparison of heart rate data (1-min average) obtained from Fitbit wearables (Fig. 2) with high-accuracy chest strap sensors (Polar A300). The 1:1 relationship is represented by a dashed line. Right: Distribution of observed core temperature as a function of heart rate. Each ID represents a unique participant in the controlled-environment experiment.

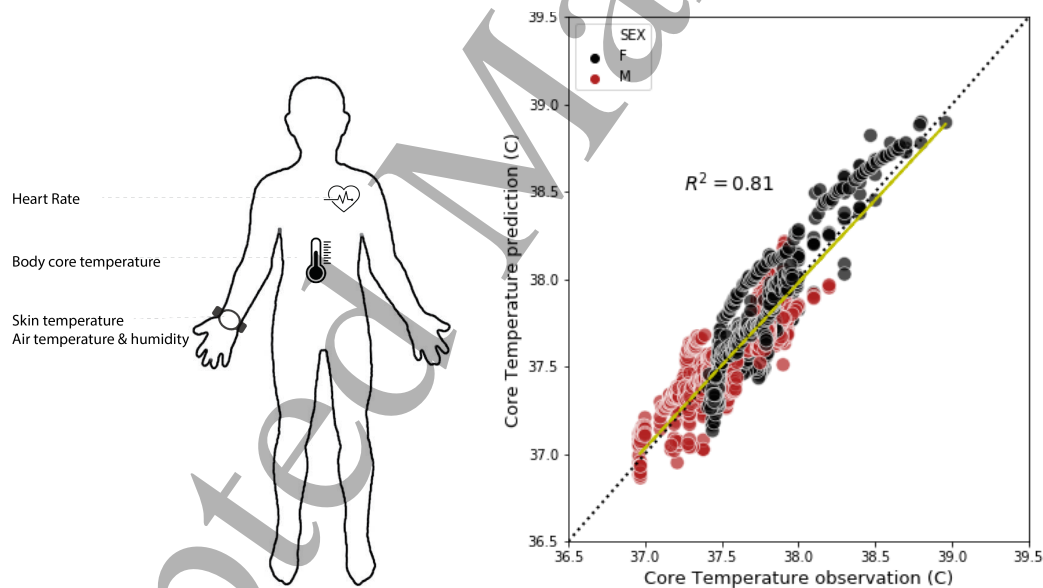


**Figure 8:** Left: schematic of various physiological and environmental parameters used to predict body core temperature, including heart rate, wrist skin temperature ( $T_{a,w}$ ) and wrist air temperature ( $T_{s,w}$ ). Skin humidity ( $RH_w$ ) was also considered in the prediction algorithm but did not increase the accuracy of results. Right: prediction of body core temperature (30-sec average) for different genders (red: male, black: female) using a Kalman filter compared with measurements in the climate chamber.

Figure 8 shows the schematic of physiological measurements for the core temperature prediction, as well as the comparison between estimated and observed  $T_c$  data. Compared to using HR as the only indicator ( $R^2 = 0.52$ , not shown), core temperature estimation is significantly improved when sequential skin and air temperature observations at wrist are used as input parameters ( $R^2 = 0.81$ ). Figure 9 shows the distribution of error and level of agreement with observations for predicted  $T_c$ . We find that 95% of the predicted core

temperature falls within  $0.27^{\circ}\text{C}$  of the measured data, which is among the best performances observed in the literature [47, 48, 52]. The mean bias and mean absolute error (MAE) are  $0.008$  and  $0.1^{\circ}\text{C}$ , respectively, with a maximum error of no more than  $0.44^{\circ}\text{C}$ . For male participants, we observe that a prediction tends to underestimate  $T_c$ , which is due to lower core temperature during the experiment as the training data. Lastly, we observe that minimum of 12-13 participants are needed to train the prediction algorithm with percentage of target attainment rate of higher than 80% (when target set as  $0.3^{\circ}\text{C}$ ) and MAE lower than  $0.25^{\circ}\text{C}$ . Overall, this analysis demonstrates the ability of wrist-mounted sensing for non-invasive prediction of core temperature and further inferring heat strain [47] and can be extended to include a larger sample size and testing with different population groups.

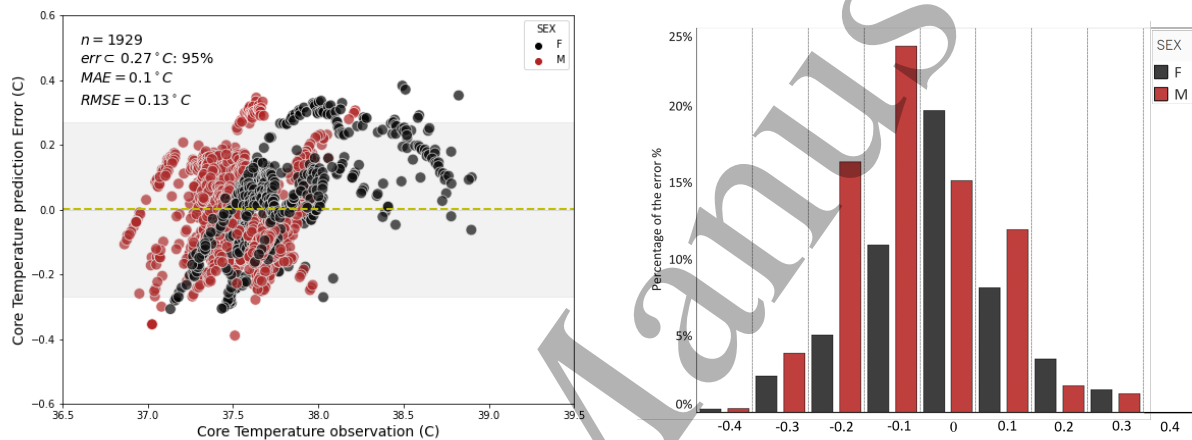


**Figure 9:** Distribution of error for predicted core temperature using a Kalman filter and sequential observed data for heart rate, air temperature, and skin temperature at wrist. Left: Bland–Altman plot of agreement between observed and predicted core temperature. 95% confidence interval is met at the target temperature error of  $0.27^{\circ}\text{C}$ . The dashed yellow line represents the bias of prediction. Right: Normalized histogram of percentage error for all training data shown based on different gender.

### 3.2 Prediction and Impacts of Thermal Sensation Vote

Comparing participants' thermal sensation with local microclimate parameters (such as WBGT obtained from fixed monitoring stations) yielded similar results to findings of Yang et al. [53] and Heng and Chow [54], indicating a linear relationship between thermal comfort indices and aggregated thermal sensation vote. Here, we extend the analysis to compare thermal sensation and satisfaction votes, TSV and TCV respectively, with data obtained from wearable devices such as skin and air temperature at the wrist (Fig. 10). We observe that thermal sensation vote (Fig. 10 - right, ranging from "Very Cold" to "Very Hot") exhibits a positive correlation with the air and skin temperature at wrist and a stronger correlation compared to ambient air temperature. For thermal comfort vote (Fig. 10 - left, ranging from "Extremely Satisfied" to "Extremely Dissatisfied"), the median and distribution of air temperature measured at the wrist exhibit the most significant correlation with thermal satisfaction, which indicates the ability of  $T_{a,w}$  for predicting comfort. Additionally, Fig. 10 shows that as TSV moves towards hotter sensations or TCV moves to higher dissatisfaction, the difference between temperatures at the wrist and ambient air temperature decreases. This difference dominates the rate of sensible heat transfer from the skin, which is critically important for human comfort and satisfaction [55].

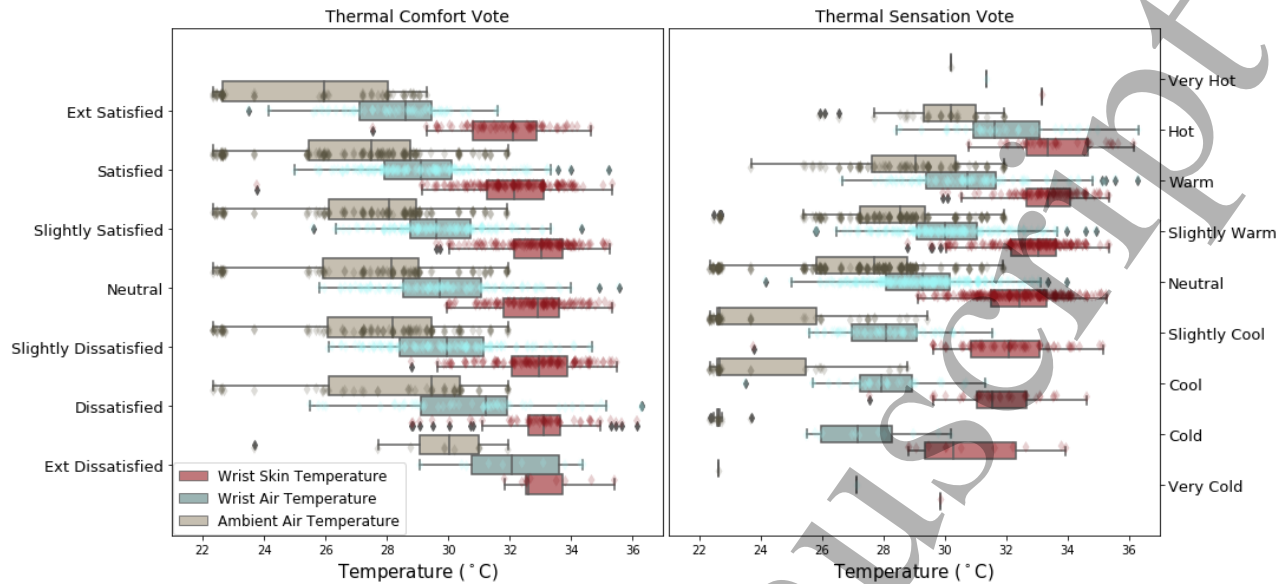


**Figure 10:** Boxplots of wrist skin temperature (red), wrist air temperature (green) and ambient air temperature (grey) categorized by Thermal Comfort Vote and Thermal Sensation Vote of participants. The boxplots are overlaid with scattered data points in each vote category. Data points represent 726 responses collected from 62 participants over 15 sessions.

Next, to analyze and predict the respondents' thermal sensation and comfort, we binned the data based on wrist air temperature ( $T_{a,w}$ ) into  $0.5\text{ }^{\circ}\text{C}$  intervals [14] and calculated the mean TSV and TCV in each bin (Fig. 11). We observe that the correlation between heart rate and TSV is weak, but skin temperature and particularly air temperature at the wrist are linearly correlated with thermal sensation. Combining measured relative humidity with air temperature obtained at the wrist [56] improved the accuracy of thermal comfort prediction (yielding  $R^2 = 0.74$  - not shown) and TSV is predicted with  $\text{MAE}=0.3$  for this dataset. However, although such prediction provides a valuable assessment of collective comfort sensation and can help to assess the impact of urban characteristics on collective dwellers' comfort, the predictive ability of such regression models for individualized response remains at  $\sim 35 - 40\%$ , in line with a range of thermal comfort indices assessed in previous studies [57]. This further motivates the development of personal comfort models [58] based on long-term data collection and consideration of behavioral and subjective factors, which is a focus in future developments of Project Coolbit.

To extend our assessment regarding the relationship between thermal sensation and satisfaction and the consequent impact on human life, we show the correlations between Thermal Comfort Vote, Thermal Sensation Vote, and Perceived Activity Vote (PAV) obtained in our experiments (Fig. 12). PAV is introduced here to assess the impact of the thermal environment on human activity and lifestyle, which is a critical factor indirectly contributing to heat-related health outcomes. For example, an uncomfortable thermal environment can result in less desire to perform physical activity, which further contributes to health challenges such as obesity, mental health, and high blood cholesterol and pressure level. Identifying such links between the thermal environment and activity level is, therefore, considered as one of the motivations and advantages of using activity-tracker wearables in this study. Assessing the perceived activity vote enables us to not only analyze and predict thermal comfort but also quantify the implications on health and wellbeing in the built environment.

In Fig. 12 (left), we observe that for the climate of Singapore, TSV corresponding to 'cool', "Slightly Cool",

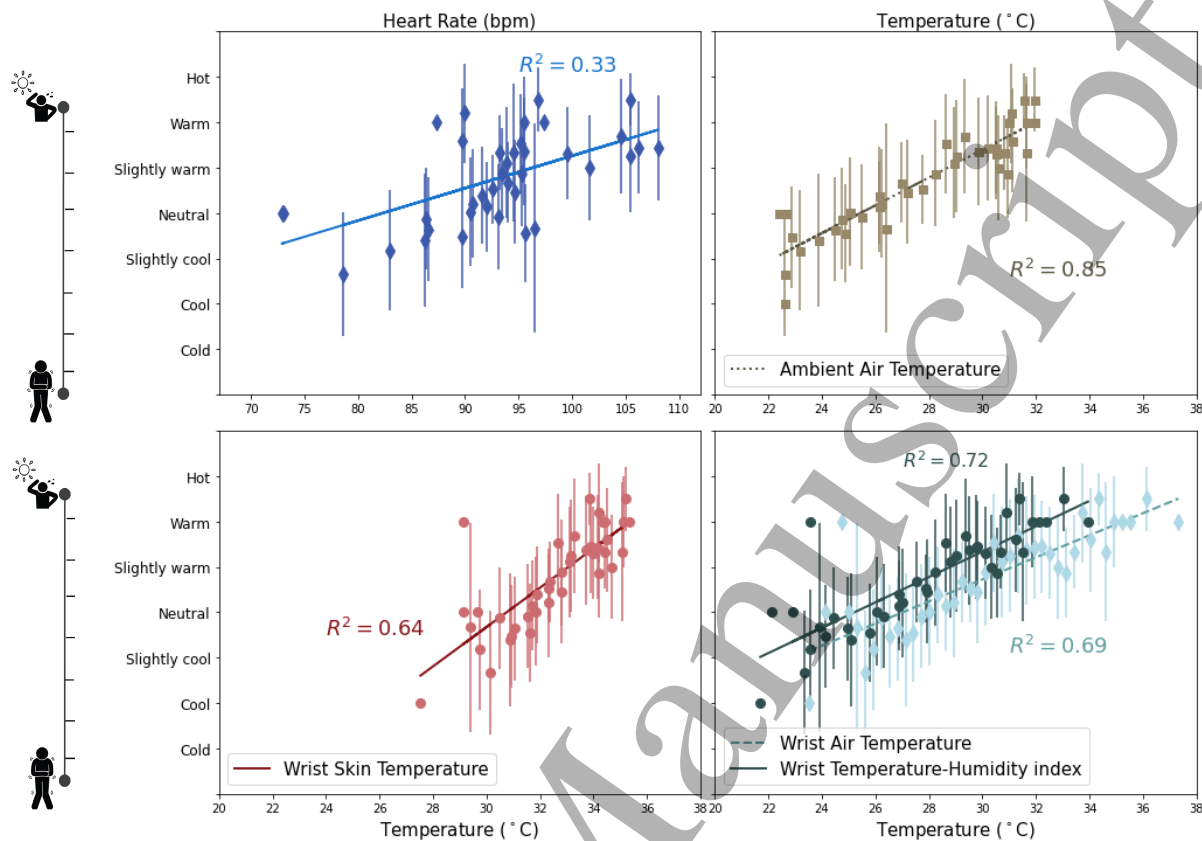


**Figure 11:** Distribution of thermal sensation vote as a function of wearable data (binned based on wrist air temperature). Pearson regression coefficient and errorbars (indicating the standard deviation of TSV for the binned data) are also presented for each variable. The temperature-humidity index is adopted from Steadman [59] to combine air temperature and relative humidity monitored at the wrist.

“Neutral” and “Slightly Warm” can lead to satisfaction of the thermal environment. This is in line with previous studies that demonstrated that a) “Neutral temperature” does not necessarily indicate thermal comfort and satisfaction [14] and b) Singapore residents tend to have a higher tolerance to colder indoor conditions, especially considering the high humidity level outdoors. More importantly, by comparing the Perceived Activity Vote with TSV (Fig. 12 - right), we find that the desire to do an activity is significantly affected by the thermal environment. Participants may be willing to do an extended activity in cold thermal sensations but a warm condition directly translated to shortened or lack of activity in our experiments. Moreover, using the binned data (Fig. 13), we can draw a direct connection between the air temperature at the wrist and perceived activity level: with increased  $T_{a,w}$ , the desire for physical activity is significantly reduced, reaching “Transition only” PAV level at  $36^{\circ}\text{C}$ . This is the first quantification of thermal comfort impact on human activity and demonstrates the ability of this methodology to not only predict the overall thermal comfort, but further contribute to quantification of the indirect impact on health through the loss of activity and change in lifestyle.

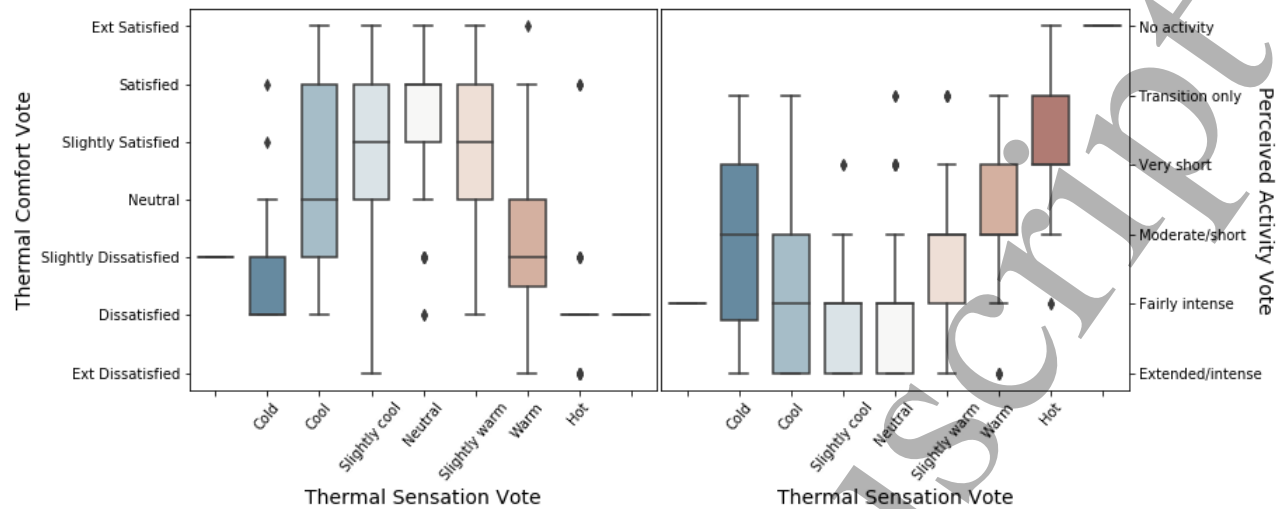


**Figure 12:** Bar charts of thermal comfort votes (TCV) as varied by thermal sensation vote (TSV) and Perceived activity vote (PAV). Results are obtained based on 720 responses of 62 participants in indoor/outdoor environments with a range of activities and built environment characteristics. For PAV, participants are asked to rank the level of activity that they perceive suitable based on the thermal environment. For example, "Extended/intense" activity indicates that participants are comfortable to perform intense activities or stay for an extended period in this thermal environment while "No activity" indicates that participants find this thermal condition extremely uncomfortable or unhealthy for any activity.

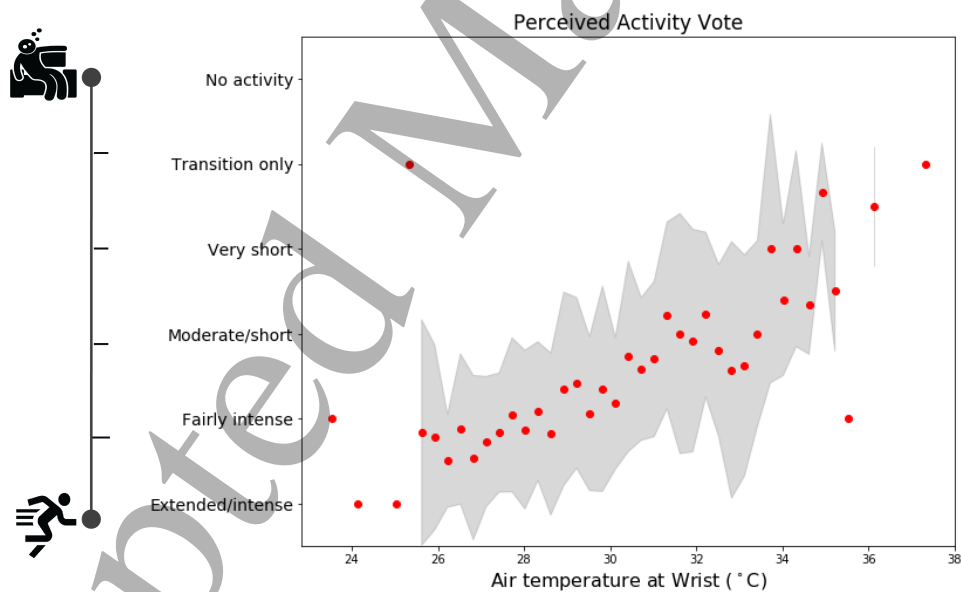


**Figure 13:** Distribution of perceived activity vote as a function of air temperature at wrist obtained from wearable sensors.

## 4 Conclusions and Future Work

Heat exposure has a wide range of adverse effects on the human body and is considered a public health hazard [5, 60]. Additionally, thermal discomfort in urban spaces has been associated with loss in productivity, cognitive performance, and wellbeing of individuals [1]. However, despite decades of climatological, epidemiological, and physiological research on this topic, little is known about actual thermal conditions people experience as they



320 go about their daily lives [61]. The personalized and real-time assessment of urban heat exposure, which  
321 further provides comprehensive assessments of impacts on human life, is yet to be achieved.

322 Such knowledge gaps and methodological limitations motivated the present study. Here, we proposed wearable  
323 sensing for human-centric heat exposure assessments, such that we connect humans with their immediate  
324 environment. We introduced an integrated personalized methodology, i.e. wearable weather stations, that  
325 in one wrist-mounted sensing unit can record environmental parameters, physiological responses, and human  
326 activities and feedback. We then addressed the feasibility of this methodology using two sets of experiments:  
327 1) controlled-environment experiments in a climate chamber focused on physiological responses and 2) semi-  
328 controlled experiments in the built environment focused on thermal comfort. The objectives were to answer  
329 two questions: *1) can this wearable sensing predict heat strain?* and *b) what information regarding thermal*  
330 *sensation can be derived using personalized monitoring?*

331 We demonstrated that body core temperature ( $T_c$ ) can be predicted non-invasively with high accuracy: using  
332 data from 15 participants,  $T_c$  was predicted using heart rate, skin temperature, and air temperature at wrist  
333 (obtained from wearable devices) and 95% of predicted results fell within  $0.27^\circ C$  of measurements obtained  
334 from telemetric capsules. This is among the best performances seen in the literature and presents the most  
335 viable option as smartwatches are easily worn and carried on the wrist at all times. However, it should be noted  
336 that due to the limited number of participants in this study (15 in total), it was not statistically meaningful to  
337 train the data using a segment of the sample size for testing and more importantly, a relatively homogeneous  
338 participant profile is considered here. Accordingly, it is critical that measurements and testings are extended  
339 to increase the number of participants with diverse profiles (such as age, gender, BMI, acclimatization status,  
340 fitness, and health conditions). We further plan to extend the measurements to higher  $T_c$  and HR ranges  
341 in collaboration With the NUS Department of Physiology and by studying healthy adults that can complete  
342 maximum physical activity tests in experimental settings.

343 Using environmental and physiological data obtained from the watch, we were also able to predict the overall  
344 sensation of participant groups. However, when regression models are applied to individualized responses,  
345 only  $\sim 35 - 40\%$  of responses are accurately predicted which is similar to previous thermal comfort models  
346 [57]. This is due to the subjective nature of thermal comfort that includes individual preferences based on  
347 behavioral, cultural, and climatic backgrounds. To account for these, we aim to extend the data collection  
348 period and employ machine learning techniques that incorporate individualized behavioral patterns to train  
349 personal comfort models [58]. More importantly, we demonstrated that this methodology can quantify the  
350 indirect impact of heat on health through the change in physical activity level and lifestyle. To the best of  
351 our knowledge, this is the first study that quantified the impact of urban heat on activity level, which opens  
352 new doors for heat-health assessments. We plan to extend this study to quantify the impacts of more realistic  
353 thermal environments on perceived and actual activity levels of individuals.

354 This study represents the first methodology to monitor personal heat exposure in a non-intrusive yet quanti-  
355 tative way, which enables us to better determine the links between climatic variables and human health and  
356 wellbeing, design effective mitigation and adaptation strategies, and prepare emergency responses to extreme  
357 conditions. Such knowledge can ultimately transform the way we understand and design for optimized ex-  
358 posure. However, we note the deployment of wearable sensors is done for a limited number of participants  
359 so far. To fully realize the impact of this methodology, the sensor array needs to be further developed and

extended in real-time and realistic conditions in the built environment, which presents a challenge regarding sensor cost and effective communication of data. Additionally, to translate this understanding to establishing climate-resilient cities, large scale deployments are needed to cover large spatial and temporal distributions in cities.

## Appendix A - Fundamentals of Kalman Filter used for Core Temperature Prediction

The Kalman filter is known for its capability of estimating unknown variables from indirect measurements that contain statistical noise and other inaccuracies. The KF model is comprised of a state-transition and an observation model, and the noise allied to each model. All the KF parameters were learned from the dataset gained in this study via linear regression. The state-transition model illustrates how the hidden variable  $T_{C,t}$  transferred from the previous time point status  $T_{C,t-1}$ , which can be defined as:

$$T_{C,t} = A \times T_{C,t-1} + A_0 + w_t \quad (1)$$

$$w_t \sim N(0, Q_t) \quad (2)$$

Where  $A$  and  $A_0$  are the weights learned by the linear regression of  $T_{C,t}$  against  $T_{C,t-1}$  with the 15 seconds time step.  $w$  is the transition model noise with a zero mean normal Gaussian distribution with covariance  $Q$ . In this case,  $Q$  is the standard deviation of minute difference of  $T_c$ .

The observation model was defined as a linear model of observed variables against the hidden variable  $T_{C,t}$ . Here we used heart rate ( $HR_t$ ), skin temperature at wrist ( $T_{sw,t}$ ), and air temperature at wrist ( $T_{aw,t}$ ) as inputs. The observation models of these two models can be represented as follows:

$$\begin{Bmatrix} HR_t \\ T_{sw,t} \\ T_{aw,t} \end{Bmatrix} = H \times T_{C,t} + H_0 + v_t \quad (3)$$

$$v_t \sim N(0, R_t) \quad (4)$$

Where  $H$  and  $H_0$  are the weight matrix learned by linear regression of  $T_c$  against  $HR$ ,  $T_{sw}$ , and  $T_{aw}$ .  $v$  is the observation model noise with a zero mean normal Gaussian distribution with covariance  $R$ .  $R$  is the covariance matrix of 15 second difference of  $HR$ ,  $T_{sw}$ , and  $T_{aw}$ .

In our analysis, at each new 15 seconds time step ( $t$ ), the KF provided a new estimate of  $T_{C,t}$  and its error variance  $P_{C,t}$  based on the observed  $HR_t$ ,  $T_{sw,t}$  and  $T_{aw,t}$  by iteratively calculating Eqs. 1 - 6. First, a preliminary estimated  $T_{C,t}$  was computed using Eqs. 1 - 2. The associated error variance was calculated as

$$P_t^T = A \times P_{t-1} \times A^T + Q_t \quad (5)$$

where the initial  $P_t$  was set as 0 and the superscript  $T$  means the transposed matrix. The Kalman gain  $K_t$  was then estimated by

$$P_t = P_t^T H^T (H P_t^T H^T + R_t)^{-1} \quad (6)$$

The final estimate of  $T_{C,t}$  was calculated with the preliminary estimate ( $T_{C,t-1}$ ), the error between the observed variables ( $HR_t$ ,  $T_{sw,t}$ , and  $T_{aw,t}$ ) and the estimated ones using the  $T_{C,t-1}$ :

$$T_{C,t} = T_{C,t}^T + K_t \begin{pmatrix} HR_t \\ T_{sw,t} \\ T_{aw,t} \end{pmatrix} - (H \times T_{C,t}^T) + H_0 \quad (7)$$

Finally, the current core temperature estimate error variance is computed as

$$P_t = (1 - K_t H) P_t^T. \quad (8)$$

## References

- [1] Fan Zhang, Richard de Dear, and Peter Hancock. Effects of moderate thermal environments on cognitive performance: A multidisciplinary review. *Appl. Energy*, 236:760–777, February 2019.
- [2] M Santamouris. Recent progress on urban overheating and heat island research. integrated assessment of the energy, environmental, vulnerability and health impact synergies with the global climate change. *Energy and Buildings*, page 109482, 2019.
- [3] S E Perkins, L V Alexander, and J R Nairn. Increasing frequency, intensity and duration of observed global heatwaves and warm spells. *Geophys. Res. Lett.*, 39(20):10, October 2012.
- [4] Will Steffen, Lesley Hughes, and Sarah Perkins. *Heatwaves: hotter, longer, more often*. Climate Council of Australia, 2014.
- [5] R Sari Kovats and Shakoor Hajat. Heat stress and public health: a critical review. *Annu. Rev. Public Health*, 29:41–55, 2008.
- [6] Iain D Stewart. Why should urban heat island researchers study history? *Urban Climate*, 30:100484, 2019.
- [7] Price Waterhouse Coopers. Protecting human health and safety during severe and extreme heat events: A national framework. *Department of Climate Change, Commonwealth Government*, 2011.
- [8] Kevin A Borden and Susan L Cutter. Spatial patterns of natural hazards mortality in the united states. *International journal of health geographics*, 7(1):64, 2008.
- [9] F Ali-Toudert and H Mayer. Thermal comfort in an east–west oriented street canyon in freiburg (germany) under hot summer conditions. *Theor. Appl. Climatol.*, 2007.
- [10] Ariane Middel and E Scott Krayenhoff. Micrometeorological determinants of pedestrian thermal exposure during record-breaking heat in tempe, arizona: Introducing the MaRTy observational platform. *Sci. Total Environ.*, 687:137–151, June 2019.
- [11] Vicky Cheng, Edward Ng, Cecilia Chan, and Baruch Givoni. Outdoor thermal comfort study in a sub-tropical climate: a longitudinal study based in hong kong. *Int. J. Biometeorol.*, 56(1):43–56, January 2012.

- 1  
2  
3 401 [12] E Johansson, S Thorsson, R Emmanuel, and E Krüger. Instruments and methods in outdoor thermal  
4 402 comfort studies—the need for standardization. *Urban climate*, 2014.
- 5  
6 403 [13] Ferdinando Salata, Iacopo Golasi, Roberto de Lieto Vollaro, and Andrea de Lieto Vollaro. Outdoor  
7 404 thermal comfort in the mediterranean area. a transversal study in rome, italy. *Build. Environ.*, 96:46–61,  
8 405 February 2016.
- 9  
10 406 [14] A Middel, N Selover, B Hagen, and N Chhetri. Impact of shade on outdoor thermal comfort—a seasonal  
11 407 field study in tempe, arizona. *International journal of*, 2016.
- 12  
13 408 [15] F Ali-Toudert and H Mayer. Numerical study on the effects of aspect ratio and orientation of an urban  
14 409 street canyon on outdoor thermal comfort in hot and dry climate. *Build. Environ.*, 2006.
- 15  
16 410 [16] Borong Lin, Xiaofeng Li, Yingxin Zhu, and Youguo Qin. Numerical simulation studies of the different  
17 411 vegetation patterns’ effects on outdoor pedestrian thermal comfort. *J. Wind Eng. Ind. Aerodyn.*, 96  
18 412 (10-11):1707–1718, 2008.
- 19  
20 413 [17] Negin Nazarian, Jipeng Fan, Tiffany Sin, Leslie Norford, and Jan Kleissl. Predicting outdoor thermal  
21 414 comfort in urban environments: A 3D numerical model for standard effective temperature. *Urban Climate*,  
22 415 20:251–267, June 2017.
- 23  
24 416 [18] Negin Nazarian, Tiffany Sin, and Leslie Norford. Numerical modeling of outdoor thermal comfort in 3D.  
25 417 *Urban Climate*, 26:212–230, December 2018.
- 26  
27 418 [19] Negin Nazarian, Juan A Acero, and Leslie Norford. Outdoor thermal comfort autonomy: Performance  
28 419 metrics for climate-conscious urban design. *Build. Environ.*, 155:145–160, May 2019.
- 29  
30 420 [20] Marialena Nikolopoulou, Nick Baker, and Koen Steemers. Thermal comfort in outdoor urban spaces:  
31 421 understanding the human parameter. *Solar Energy*, 70(3):227–235, January 2001.
- 32  
33 422 [21] Peter Höpfe. Different aspects of assessing indoor and outdoor thermal comfort. *Energy Build.*, 34(6):  
34 423 661–665, July 2002.
- 35  
36 424 [22] Liang Chen and Edward Ng. Outdoor thermal comfort and outdoor activities: A review of research in  
37 425 the past decade. *Cities*, 29(2):118–125, April 2012.
- 38  
39 426 [23] Xuping Song, Shigong Wang, Yuling Hu, Man Yue, Tingting Zhang, Yu Liu, Jinhui Tian, and Kezheng  
40 427 Shang. Impact of ambient temperature on morbidity and mortality: an overview of reviews. *Science of*  
41 428 *the Total Environment*, 586:241–254, 2017.
- 42  
43 429 [24] Lee Chapman, Cassandra Bell, and Simon Bell. Can the crowdsourcing data paradigm take atmospheric  
44 430 science to a new level? a case study of the urban heat island of london quantified using netatmo weather  
45 431 stations: CROWDSOURCING THE LONDON UHI. *Int. J. Climatol.*, 37(9):3597–3605, July 2017.
- 46  
47 432 [25] Makoto Nakayoshi, Manabu Kanda, Rui Shi, and Richard de Dear. Outdoor thermal physiology along  
48 433 human pathways: a study using a wearable measurement system. *Int. J. Biometeorol.*, 59(5):503–515,  
49 434 May 2015.
- 50  
51 435 [26] Shichao Liu, Stefano Schiavon, Hari Prasanna Das, Ming Jin, and Costas J Spanos. Personal thermal  
52 436 comfort models with wearable sensors. *Building and Environment*, 162:106281, 2019.

- 1  
2  
3 437 [27] Satoru Takada, Sho Matsumoto, and Takayuki Matsushita. Prediction of whole-body thermal sensation  
4 438 in the non-steady state based on skin temperature. *Build. Environ.*, 68:123–133, October 2013.
- 5  
6 439 [28] Soo Young Sim, Myung Jun Koh, Kwang Min Joo, Seungwoo Noh, Sangyun Park, Youn Ho Kim, and  
7 440 Kwang Suk Park. Estimation of thermal sensation based on wrist skin temperatures. *Sensors*, 16(4):420,  
8 441 March 2016.
- 9  
10 442 [29] Mark J Buller, William J Tharion, Samuel N Cheuvront, Scott J Mountain, Robert W Kenefick, John  
11 443 Castellani, William A Latzka, Warren S Roberts, Mark Richter, Odest Chadwicke Jenkins, and Reed W  
12 444 Hoyt. Estimation of human core temperature from sequential heart rate observations. *Physiol. Meas.*, 34  
13 445 (7):781–798, July 2013.
- 14  
15  
16 446 [30] Moatassef Abdallah, Clevenger Caroline, Vu Tam, and Nguyen Anh. Sensing occupant comfort using  
17 447 wearable technologies. *Construction Research Congress 2016*, 2016.
- 18  
19  
20 448 [31] International Data Corporation. Worldwide quarterly: wearable device tracker. 2015.
- 21  
22 449 [32] Michael N Sawka and Karl E Friedl. Emerging wearable physiological monitoring technologies and decision  
23 450 aids for health and performance. *J. Appl. Physiol.*, 124(2):430–431, February 2018.
- 24  
25 451 [33] Karl E Friedl, Mark J Buller, William J Tharion, Adam W Potter, Glen L Manglapus, and Reed W  
26 452 Hoyt. Real time physiological status monitoring (RT-PSM): accomplishments, requirements, and research  
27 453 roadmap. Technical report, ARMY RESEARCH INST OF ENVIRONMENTAL MEDICINE NATICK  
28 454 MA BIOPHYSICS AND . . . , 2016.
- 29  
30  
31 455 [34] Mark J Buller, Alexander P Welles, and Karl E Friedl. Wearable physiological monitoring for human  
32 456 thermal-work strain optimization. *J. Appl. Physiol.*, 124(2):432–441, February 2018.
- 33  
34 457 [35] Fitbit, Inc. Fitbit official site for activity trackers. <https://www.fitbit.com/au/home>. Accessed: 2019-  
35 458 7-9.
- 36  
37 459 [36] Yang Bai, Paul Hibbing, Constantine Mantis, and Gregory J Welk. Comparative evaluation of heart  
38 460 rate-based monitors: Apple watch vs fitbit charge hr. *Journal of sports sciences*, 36(15):1734–1741, 2018.
- 39  
40 461 [37] Shahab Haghayegh, Sepideh Khoshnevis, Michael H Smolensky, and Kenneth R Diller. Accuracy of  
41 462 PurePulse photoplethysmography technology of fitbit charge 2 for assessment of heart rate during sleep.  
42 463 *Chronobiol. Int.*, 36(7):927–933, July 2019.
- 43  
44 464 [38] Maxim Integrated. Overview of ibutton® sensors and Temperature/Humidity data loggers - applica-  
45 465 tion note - maxim. <https://www.maximintegrated.com/en/app-notes/index.mvp/id/3892>. Accessed:  
46 466 2019-7-9.
- 47  
48  
49 467 [39] P Jayathissa, M Quintana, T Sood, N Nazarian, and C Miller. Is your clock-face cozie? a smartwatch  
50 468 methodology for the in-situ collection of occupant comfort data. *J. Phys.: Conf. Ser.*, 1343(012145), 2019.
- 51  
52 469 [40] Philips Respironics. VitalSense Telemetric Physiological Monitoring System. <http://www.actigraphy.com/solutions/vitalsense/>. Accessed: 2019-7-10.  
53 470
- 54  
55 471 [41] NL Ramanathan. A new weighting system for mean surface temperature of the human body. *Journal of*  
56 472 *applied physiology*, 19(3):531–533, 1964.

- 1  
2  
3 473 [42] Gunnar Borg. Psychophysical scaling with applications in physical work and the perception of exertion.  
4 474 *Scand J Work Environ Health*, 16(Suppl 1):55–58, 1990.
- 5  
6 475 [43] Negin Nazarian, Clayton Miller, Leslie Norford, Manon Kohler, Winston Chow, Jason Lee Kai Wei,  
7 476 Sharifah Badriyah Alhadad, Matias Quintana, Lindsey Sunden, and Alberto Martilli. Project coolbit  
8 477 updates: Personal thermal comfort assessments using wearable devices. In *Geophysical Research Abstracts*,  
9 478 volume 21, 2019.
- 10  
11  
12 479 [44] A Pharo Gagge and Yasunobu Nishi. Heat exchange between human skin surface and thermal environ-  
13 480 ment. *Comprehensive Physiology*, pages 69–92, 2010.
- 14  
15 481 [45] Weiwei Liu, Zhiwei Lian, Qihong Deng, and Yuanmou Liu. Evaluation of calculation methods of mean  
16 482 skin temperature for use in thermal comfort study. *Building and Environment*, 46(2):478–488, 2011.
- 17  
18 483 [46] Jason KW Lee, Amanda QX Nio, Chin Leong Lim, Eunice YN Teo, and Christopher Byrne. Ther-  
19 484 moregulation, pacing and fluid balance during mass participation distance running in a warm and humid  
20 485 environment. *European journal of applied physiology*, 109(5):887–898, 2010.
- 21  
22  
23 486 [47] Mark J Buller, William J Tharion, Samuel N Cheuvront, Scott J Montain, Robert W Kenefick, John  
24 487 Castellani, William A Latzka, Warren S Roberts, Mark Richter, Odest Chadwicke Jenkins, et al. Esti-  
25 488 mation of human core temperature from sequential heart rate observations. *Physiological measurement*,  
26 489 34(7):781, 2013.
- 27  
28  
29 490 [48] David P Looney, Mark J Buller, Andrei V Gribok, Jayme L Leger, Adam W Potter, William V Rumpler,  
30 491 William J Tharion, Alexander P Welles, Karl E Friedl, and Reed W Hoyt. Estimating resting core  
31 492 temperature using heart rate. *Journal for the Measurement of Physical Behaviour*, 1(2):79–86, 2018.
- 32  
33  
34 493 [49] Rudolph Emil Kalman. A new approach to linear filtering and prediction problems. *Journal of basic*  
35 494 *Engineering*, 82(1):35–45, 1960.
- 36  
37 495 [50] Mark J Buller, William J Tharion, Reed W Hoyt, and Odest Chadwicke Jenkins. Estimation of human  
38 496 internal temperature from wearable physiological sensors. In *Twenty-Second IAAI Conference*, 2010.
- 39  
40 497 [51] Kok-Yong Seng, Ying Chen, Kian Ming A Chai, Ting Wang, David Chiok Yuen Fun, Ya Shi Teo, Pearl  
41 498 Min Sze Tan, Wee Hon Ang, and Jason Kai Wei Lee. Tracking body core temperature in military  
42 499 thermal environments: An extended kalman filter approach. In *2016 IEEE 13th International Conference*  
43 500 *on Wearable and Implantable Body Sensor Networks (BSN)*, pages 296–299. IEEE, 2016.
- 44  
45  
46 501 [52] Alexander P Welles, Xiaojiang Xu, William R Santee, David P Looney, Mark J Buller, Adam W Potter,  
47 502 and Reed W Hoyt. Estimation of core body temperature from skin temperature, heat flux, and heart  
48 503 rate using a kalman filter. *Computers in biology and medicine*, 99:1–6, 2018.
- 49  
50 504 [53] Wei Yang, Nyuk Hien Wong, and Steve Kardinal Jusuf. Thermal comfort in outdoor urban spaces in  
51 505 singapore. *Building and Environment*, 59:426–435, 2013.
- 52  
53  
54 506 [54] Su Li Heng and Winston TL Chow. How ‘hot’ is too hot? evaluating acceptable outdoor thermal comfort  
55 507 ranges in an equatorial urban park. *International journal of biometeorology*, 63(6):801–816, 2019.
- 56  
57 508 [55] Edward A Arens and H Zhang. The skin’s role in human thermoregulation and comfort. 2006.
- 58  
59  
60

- 1  
2  
3 509 [56] Earl Crabill Thom. The discomfort index. *Weatherwise*, 12(2):57–61, 1959.
- 4  
5 510 [57] María Angélica Ruiz and Erica Norma Correa. Suitability of different comfort indices for the prediction  
6 511 of thermal conditions in tree-covered outdoor spaces in arid cities. *Theoretical and applied climatology*,  
7 512 122(1-2):69–83, 2015.
- 8  
9 513 [58] Joyce Kim, Yuxun Zhou, Stefano Schiavon, Paul Raftery, and Gail Brager. Personal comfort models:  
10 514 predicting individuals' thermal preference using occupant heating and cooling behavior and machine  
11 515 learning. *Building and Environment*, 129:96–106, 2018.
- 12  
13  
14 516 [59] Robert G Steadman. The assessment of sultriness. part i: A temperature-humidity index based on human  
15 517 physiology and clothing science. *Journal of applied meteorology*, 18(7):861–873, 1979.
- 16  
17 518 [60] Peng Bi, Susan Williams, Margaret Loughnan, Glenis Lloyd, Alana Hansen, Tord Kjellstrom, Keith  
18 519 Dear, and Arthur Saniotis. The effects of extreme heat on human mortality and morbidity in australia:  
19 520 implications for public health. *Asia. Pac. J. Public Health*, 23(2 Suppl):27S–36, March 2011.
- 20  
21 521 [61] Evan R Kuras, Molly B Richardson, Miriam M Calkins, Kristie L Ebi, Jeremy J Hess, Kristina W  
22 522 Kintziger, Meredith A Jagger, Ariane Middel, Anna A Scott, June T Spector, Christopher K Uejio,  
23 523 Jennifer K Vanos, Benjamin F Zaitchik, Julia M Gohlke, and David M Hondula. Opportunities and  
24 524 challenges for personal heat exposure research. *Environ. Health Perspect.*, 125(8):085001, August 2017.
- 25  
26  
27  
28  
29  
30  
31  
32  
33  
34  
35  
36  
37  
38  
39  
40  
41  
42  
43  
44  
45  
46  
47  
48  
49  
50  
51  
52  
53  
54  
55  
56  
57  
58  
59  
60